Luminescence spectra of quantum dots in microcavities. I. Bosons

Fabrice P. Laussy*
School of Physics and Astronomy, University of Southampton, Southampton SO17 1BJ, United Kingdom

Elena del Valle and Carlos Tejedor
Departamento de Física Teórica de la Materia Condensada, Universidad Autónoma de Madrid, 28049 Madrid, Spain

(Received 12 June 2008; revised manuscript received 5 May 2009; published 23 June 2009)

We provide a unified theory of luminescence spectra of coupled light-matter systems realized with semiconductor heterostructures in microcavities, encompassing (i) the spontaneous emission case, where the system decays from a prepared (typically pure) initial state, and (ii) luminescence in the presence of a continuous incoherent pump. We show how, by provoking a self-consistent quantum state, the pump considerably alters the emission spectra, even at vanishing intensities. The main outcome of our analysis is to unambiguously identify strong coupling in situations where it appears in disguise or only seems to appear. Here, we consider bosonic matter fields, in which case fully analytical solutions can be obtained. This describes the case of quantum wells or large quantum dots, or the limit of low excitation where the probability to have particles in the system remains much smaller than one.

DOI: 10.1103/PhysRevB.79.235325 PACS number(s): 42.50.Ct, 78.67.Hc, 42.55.Sa, 32.70.Jz

I. INTRODUCTION

The dynamics of an optical emitter changes drastically when it is placed in a cavity. The cavity alters the density of states of optical modes, and therefore increases or inhibits interactions with the emitter. The effect was first put to use by Purcell in nuclear magnetic resonance for the practical purpose of thermalizing spins at radio frequencies, by bringing down their relaxation time from $\approx 10^{21}$ s to a few minutes.[1] Kleppner applied the same idea in the opposite way to increase the relaxation time of an excited atom, i.e., to inhibit its spontaneous emission (SE).[2] The emitter, which in the case of Purcell was sought to be resonant with the cavity mode to increase the photon density of states with respect to the vacuum, was in the case of Kleppner put out of resonance, namely, in a photonic gap, where the photon density of states is smaller than in vacuum. This tuning of the relaxation time of an emitter placed in a cavity, now known as the *Purcell effect*, has many potential technological applications; one of the most compelling is the decrease in the lasing threshold. The effect, which had first been actively looked for with atoms in cavities,[3] was therefore also intensively (and more recently) pursued in the solid state, more prone for massive technological implementations. Semiconductor heterostructures are the state-of-the-art arena for this purpose. They allow one to engineer, with an ever rising control, the solid-state counterpart of the atomic system to match or isolate their excitation spectra and thus control their behavior. Typical examples are quantum dots (QDs) placed in cavities made in micropillars, microdisks, or photonic crystals, where Purcell inhibition has been distinctly demonstrated.[4,5] A few reviews have appeared on this topic.[6,7] In this paper, we shall be concerned chiefly with the observed spectra of emission of such an emitter placed in a cavity. In the regime where the effect of the cavity is to lengthen or shorten the lifetime of the excitation, the consequence in the optical spectra is to narrow or broaden the line, respectively.

In the description of the Purcell effect, the possible reabsorption of the photon by the emitter is so weak that it can be neglected. It is responsible for the energy shift known as the Lamb shift that, in quantum electrodynamics, is interpreted as the perturbative influence of virtual photons emitted and reabsorbed by the emitter. In the case of inhibition of the spontaneous emission, this shift is indeed orders of magnitude smaller than the radiative broadening. In the case where emission is enhanced, and the linewidth narrowed, the probability of reabsorption of a photon by the emitter becomes closer to that of escaping the cavity, until the perturbative—so-called *weak coupling* (WC)—regime breaks down and instead *strong coupling* (SC) takes place. In this case, photons emitted are then reflected by the mirrors and there is a higher probability for their reabsorption by the atom than for their leaking out of the cavity. A whole sequence of absorptions and emissions can therefore take place, known as *Rabi oscillations*. This regime is of greater interest, as it gives rise to new quantum states of the light-matter coupled system, usually referred to as *dressed states* in atomic physics and as *polaritons* in solid-state physics. Experimentally, SC is more difficult to reach, as it requires a fine control of the quantum coupling between the bare modes and in particular to reduce, as much as possible, all the sources of dissipation. Theoretically, it is better dealt with by first getting rid of the dissipation, and starting with the *strong-coupling Hamiltonian* ($\hbar$ is taken as 1 along the paper)

$$H = \omega_a a^\dagger a + \omega_b b^\dagger b + g(a^\dagger b + a b^\dagger), \tag{1}$$

where a and b are the cavity photon and material excitation field operators, respectively, with bare mode energies ω_a and ω_b, coupled linearly with strength g. The photon operator is a Bose annihilation operator, satisfying the usual commutation rule $[a,a^\dagger]=1$. Depending on the model for the material excitation, b is described by, typically, another harmonic oscillator (*linear model*[8]) or a two-level system (*Jaynes-Cummings model*[9]). Those are the most fundamental cases as they describe material fields with Bose and Fermi statistics, respectively. Possible extensions are a collection of harmonic oscillators[10] or of two-level systems,[11] a three-level system,[12]

etc. This paper contains the first part of our work in which we address exclusively the case where b also follows Bose statistics and the energy of an excitation is independent of the manifold. This is an important case for two reasons. The first one is that in many relevant cases, the matter field is indeed bosonic, such as the case of quantum wells, or large quantum dots, at low density of excitations. The second reason is that this case provides the limit for vanishing excitations (*linear limit*) of all the other cases and is fully solvable analytically. As such, this case serves as the backbone for the qualitative understanding of SC. In the second part of this work,[13] we investigate the case of fermionic behavior at large pumping, more relevant when dealing with small QDs that confine excitations and more prone to involve genuine quantum mechanics as one quantum of excitation can alter the system response. The drawback is that numerical computation is required in this case, and the discussion is therefore of a somehow less fundamental character.

For the rest of the text, it is therefore understood that b is also a Bose operator. For convenience, we shall refer to it as the *exciton* operator, after the name of a bound electron-hole pair in a semiconductor. Likewise, we shall prefer such terminology as a QD rather than an atom, or polaritons, rather than dressed states, etc. For most purposes, this is semantics only and the results apply in a wide range of systems.

Equation (1) can be straightforwardly diagonalized for bosonic modes, giving $H=\omega_U p^\dagger p+\omega_L q^\dagger q$, where

$$\omega_{\substack{U\\L}} = \frac{\omega_a+\omega_b}{2} \pm \sqrt{g^2+\left(\frac{\Delta}{2}\right)^2}, \tag{2}$$

with new Bose operators $p=\cos\theta a+\sin\theta b$ and $q=-\sin\theta a+\cos\theta b$, determined by the *mixing angle*, $\theta=\arctan[g/(\frac{\Delta}{2}+\sqrt{g^2+(\frac{\Delta}{2})^2})]$, and the detuning

$$\Delta = \omega_a - \omega_b. \tag{3}$$

These new modes are the polaritons (or dressed states) with quantum states $|U\rangle=p^\dagger|\text{vac}\rangle=\cos\theta|1,0\rangle+\sin\theta|0,1\rangle$ and $|L\rangle=q^\dagger|\text{vac}\rangle=-\sin\theta|1,0\rangle+\cos\theta|0,1\rangle$, where $|\text{vac}\rangle$ is the vacuum, $|1,0\rangle$ is the Fock state of one photon, and $|0,1\rangle$ is the Fock state of one exciton. Polariton energies [in Eq. (2)] do not depend on the manifold of excitation. This is a fundamental difference with the two-level description for the exciton[13] or with the inclusion of interactions.[14]

The energies defined by Eq. (2) are displayed in Fig. 1 with dashed lines, on top of that of the bare modes, with thick lines, as detuning is varied by changing the energy of the emitter and keeping that of the cavity constant. The *anticrossing* always keeps the upper mode, U, higher in energy than the lower one, L, strongly admixing the light and matter character of both particles. At resonance, this mixing is maximal,

$$\left|\begin{matrix}U\\L\end{matrix}\right\rangle = \frac{1}{\sqrt{2}}(|0,1\rangle \pm |1,0\rangle). \tag{4}$$

If the system is initially prepared as a bare state—which is the natural picture when reaching the SC from the excited state of an emitter—the dynamics is that of an oscillatory transfer of energy between light and matter. In an empty cavity, the time evolution of the probability to have an exciton when there was initially one (at $t=0$) reads

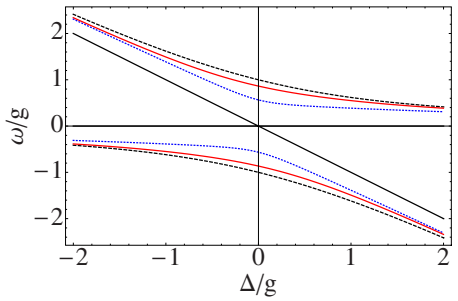

FIG. 1. (Color online) Solid black: bare energies of the cavity photon (horizontal line) and of the exciton (tilted) as a function of detuning Δ. Dashed black: eigenenergies of the system Hamiltonian, without dissipation nor pumping [Eq. (2)]. The excitonlike state at large negative Δ has become a photonlike state at large positive Δ, and vice versa. Around $\Delta=0$, both modes are an admixture of exciton and photon. Dotted blue: Correction of the eigenenergies when pump and decay are taken into account for parameters of point (c) in Fig. 8. Solid red: actual position of the observed peaks in the photoluminescence (PL) spectra for the same parameters. For these parameters, the three descriptions of SC give the same qualitative results.

$$|\langle 0,1|e^{-iHt}|0,1\rangle|^2 = \sin^4\theta + \cos^4\theta + 2\sin^2\theta\cos^2\theta\cos[(\omega_U-\omega_L)t]. \tag{5}$$

The probability oscillates between the bare modes at the so-called *Rabi frequency*, given by the difference between the polariton energies $\omega_U-\omega_L$. For convenience of notation, we will deal in what follows with half of this quantity:

$$\mathcal{R} = \frac{\omega_U-\omega_L}{2} = \sqrt{g^2+\left(\frac{\Delta}{2}\right)^2}. \tag{6}$$

The *emission spectrum* of the system requires dissipation, as it is an obvious practical requisite that the excitation should eventually leak out of the system to be detected from the outside [the *energy spectrum* of the system is given by Eq. (2)]. Dissipation is intrinsic to the bare modes; both the cavity photon and the exciton have a finite lifetime. In presence of dissipation, the system is upgraded from a Hamiltonian description, Eq. (1), to a Liouvillian description, with a quantum dissipative master equation for the density matrix ρ defined in the tensor product of the light and matter Hilbert spaces $\mathcal{H}_a$ and $\mathcal{H}_b$,[15]

$$\partial_t\rho = \mathcal{L}_\gamma\rho. \tag{7}$$

The Liouvillian $\mathcal{L}_\gamma$ still contains the Hamiltonian dynamics of SC but also takes into account the decays of both the cavity and the emitter, with rates γ_a and γ_b, respectively,

$$\mathcal{L}_\gamma\rho = i[\rho,H] + \sum_{c=a,b}\frac{\gamma_c}{2}(2c\rho c^\dagger - c^\dagger c\rho - \rho c^\dagger c), \tag{8}$$

in which we have considered the temperature equal to 0. This equation has been extensively studied,[16] although not in its most general form. The typical configuration addresses the

case of resonance, $\omega_a = \omega_b$, with only one particular initial condition, namely, the excited state of the emitter in an empty cavity, and detecting the emission of the emitter itself. All together, they describe the spontaneous emission of an emitter placed into a cavity with which it enters into SC. This has been the topical case for decades as this was the case of experimental interest with atoms in cavities.

With the advent of SC in other systems, other configurations start to be of interest. With a QD in a microcavity, the *detuning* Δ between the modes, Eq. (3), is a crucial experimental parameter, as it can be easily tuned and to a great extent, for instance by applying a magnetic field or changing the temperature. Also in this case, the detection is in the optical mode of the cavity rather than the direct emission of the exciton emission because the latter is awkward for various technical reasons of a more or less fundamental character (an example of a fundamental complication is that the emission is enhanced in the cavity mode and suppressed otherwise, and the exciton lifetime is typically much longer, so the exciton emission is much weaker; an example of a petty technical complication, e.g., with a pillar microcavity, is that the exciton detection should be made at an angle and, practically, a lot of samples are grown on the same substrate. Both the substrates and other samples hinder the lateral access to one given sample, whereas all are equally accessible from above. Photonic crystals also present difficulties related to their geometry). In our system where both modes are bosonic, symmetry allows us to focus on the cavity emission without loss of generality, as we can obtain the leaky excitonic emission by simply exchanging indexes a,b (the spectrum could also have photon-exciton crossed terms that could be computed in a similar way). When we shall turn to the case of a fermionic matter field, where the exciton emission will become distinctly different and for that reason, important, we shall address exciton emission separately.[13]

Regarding the initial condition, more general quantum states can now be realized, at least in principle, by coherent control, pulse shaping, or similar techniques. Additionally and more importantly, the type of excitation of a cavity-emitter system in a semiconductor is of a different character; the excitation is typically injected by either a continuous-wave (cw) laser far above resonance, creating electron-hole pairs that relax incoherently to excite the QD in a continuous flow of excitations, or by electrical pumping, as in lasers. This pumping, which is of an incoherent nature typical of semiconductor physics, brings many fundamental changes into the problem that go beyond the mere generalization of Eq. (8). Among the most obvious ones, let us already mention that pure states of the like of Eq. (4) do not correspond to the experimental reality. Instead, the system is maintained in a mixed state with probabilities $p(n)$ to realize the nth excited state. In all cases, a steady state (SS) is imposed by the interplay of pumping and decay. The Rabi oscillations of the populations—that is, the coherent exchange of energy between the modes—are washed out, regardless of the photonlike, excitonlike, or polaritonlike (eigenstate) character of the density matrix.

There have been naturally many efforts and a large output in the literature to describe theoretically light-matter coupling in a semiconductor microcavity. A huge majority addressed the spontaneous emission case partly because of the precedent set up by the atomic case. First results were obtained for polaritons in planar cavities, where SC was first realized.[17] Pau *et al.*[18] described the spectra of microcavity polaritons in the very strong-coupling regime (in a Lorentzian limit). Savona *et al.*[19] outlined the importance of which measurement is being performed in assessing a Rabi splitting, deriving different expressions for the observed splittings in reflection, transmission, absorption, and photoluminescence, which are ultimately related to the channel of detection in the zero-dimensional (0D) problem.[20] In the quantum dot case, Andreani *et al.*[21] opened the field, relying on the atomic theory.[16] Their major contribution was the analysis of the coupling strength g and the prediction of QDs in microcavities as successful candidates for SC physics. However, the expression for the luminescence spectrum, which was taken straight from the atomic literature, concerned the configuration of direct exciton emission, which is not the canonical case of a semiconductor microcavity where photons are detected through their leakage in the cavity mode. This was addressed by Cui and Raymer,[22] who computed the spectra both in the forward and the side emission. They also focused on the role of pure dephasing, which role out of resonance was highlighted after their model[23] or with a master equation.[24] Based on the Green's function approach, Hughes and Yao also computed the spectral lines in both geometries, but accounting for their interferences that, interestingly, can give rise to a triplet structure in the cavity emission.[25] Let us also mention, among the numerous recent works on the SE of an excited state in a cavity, Auffèves *et al.*[26] and Inoue *et al.*,[27] who gave an insightful description of the resonances that appear in these systems, prone to interferences in peculiar configurations. All these results correspond to the spontaneous emission of one excitation. We postpone the overview of works that probe the higher manifolds of the Jaynes-Cummings to part II of this work.[13]

Here, we address both the emission spectra obtained in a configuration of SE—where an initial state is prepared and left to decay, as ruled by Eqs. (7) and (8)—under its most general setting, and the case of luminescence emission under the action of a continuous and incoherent pumping that establishes a SS. We bring all the results under a common and unified formalism and show how none of the cases fully encompasses the other. We focus especially on the continuous pumping case which endows the problem with self-consistency in view of its initial state. The rest of this paper is organized as follows. In Sec. II, we present the complete model and we derive and discuss its equation of motion. In Sec. III, we analyze the single-time dynamics. In Sec. IV, we obtain fully analytically the main results in both of the cases explicated above, this time focusing more on the two-time dynamics, which Fourier transform gives the luminescence spectra. In Sec. V, we discuss the mathematical results derived in the two previous sections, accentuating the physical picture and relying on particular cases for illustration. In this section, we consider specifically the case of resonance, where all the concepts manifest more clearly. Finally, in Sec. VI, we give a summary of the main results and provide an index of all the important formulas and key figures of this text. We conclude with a short overview of the continuation

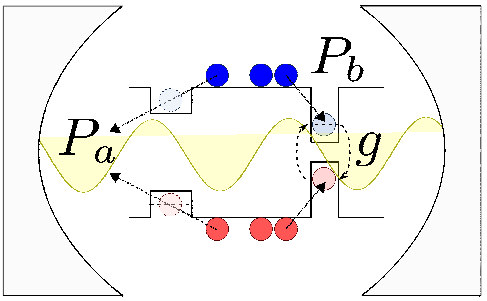

FIG. 2. (Color online) Schema of our system for the SS case: self-assembled QDs in a semiconductor microcavity. The QD sketched on the right is in SC with the cavity mode with coupling strength g, while the one of the left is in WC. The electron-hole pairs created by the incoherent pumping of the structure provide an effective electronic pumping, P_b, of the SC dot, while the pumping of the WC dot results in an effective cavity pumping P_a, through rapid conversion of the excitons into cavity photons.

of this work that replaces the bosonic emitter with a fermionic one.

II. MODEL

Our model for the coupling of a QD with a single cavity mode in the presence of incoherent and continuous pumping is sketched in Fig. 2. One QD is strongly coupled to the cavity mode with interaction strength g and is continuously, and incoherently, excited by an electronic pumping P_b, which, in the microscopic picture, is linked to the rate at which electron-hole pairs relax into the dot. This rate is related in some way to the pumping exerted by the experimentalist. Because of the incoherent nature of this pumping, together with that of the damping, the off-diagonal elements of the QD reduced density matrix (that hold the coherence) are washed out in the SS. We also consider another type of pumping, P_a, that offers a counterpart for the cavity by injecting photons incoherently at this rate. A likely factor to account for such a term is the presence of many other QDs that have been grown along with the one of interest. Those only interact weakly with the cavity. In most experimental situations so far, it is indeed difficult to find one dot with a sufficient coupling to enter the nonperturbative regime. When this is the case, all the other dots that remain in WC become *spectators* of the SC physics between the interesting dot and the cavity, and their presence is noticed by weak emission lines in the luminescence spectrum and an increased cavity emission. They are also excited by the electronic pumping that is imposed by the experimentalist, but instead of undergoing SC, they relax their energy into the cavity by Purcell enhancement or inhibition, depending on their proximity with the cavity mode. This, in turn, results in an effective pumping of the cavity.[28]

To model these two continuous and incoherent pumping, we use the Lindblad terms $\mathcal{L}_P$ that substitute the annihilation operator c (standing for a or b) by the creation one $c^\dagger$, and vice versa, a procedure which is known to describe pumping terms in a quantum rate equation.[29] Another approach with a microscopic derivation of the pumping mechanism has been recently investigated.[30] The full Liouvillian in our case then reads (again at zero temperature)

$$\partial_t \rho = \mathcal{L}\rho = i[\rho, H] \tag{9a}$$

$$+ \sum_{c=a,b} \frac{\gamma_c}{2}(2c\rho c^\dagger - c^\dagger c\rho - \rho c^\dagger c) \tag{9b}$$

$$+ \sum_{c=a,b} \frac{P_c}{2}(2c^\dagger \rho c - cc^\dagger \rho - \rho cc^\dagger). \tag{9c}$$

The microscopic derivation of line (9c) follows from the usual Born-Markov approximation.[15] The case of electronic pumping, for instance, is similar to the process of laser gain; the medium requires an inversion of electron-hole population, something that cannot be achieved by means of a simple harmonic-oscillator heat bath. The actual process of gaining an exciton in the QD involves the annihilation of an electron-hole pair in an external reservoir out of equilibrium (representing either electrical injection or the capture of excitons optically created at frequencies larger than the ones of our system) and the emission of a phonon, which carries the excess of energy, to another one (which can be in thermal equilibrium). A simple effective description of this nonequilibrium process can be made by an inverted harmonic oscillator with levels $E_p = -\omega_P(p+1/2)$ maintained at a *negative temperature*.[29] Since the raising operator for the energy decreases the number of quanta of this oscillator, the role of creation and destruction operators is indeed reversed with respect to the usual case of damping.

For the sake of generality, we introduce *effective broadenings*, which reduce to the decay rates in the SE case but get renormalized by the pumping rate in the SS case,

$$\Gamma_{a,b} = \gamma_{a,b} \quad \text{(SE case)}, \tag{10a}$$

$$\Gamma_{a,b} = \gamma_{a,b} - P_{a,b} \quad \text{(SS case)}. \tag{10b}$$

We shall also use thoroughly the combinations

$$\gamma_\pm = \frac{\gamma_a \pm \gamma_b}{4} \quad \text{and} \quad \Gamma_\pm = \frac{\Gamma_a \pm \Gamma_b}{4}. \tag{11}$$

The narrowing of the linewidth in the presence of the pumping term is a bosonic effect. In the case of a single harmonic oscillator driven by pump and decay, the emission spectrum is a Lorentzian line shape with full width at half maximum given by $\gamma - P = \gamma/(1+\langle n\rangle)$. The linewidth narrows with the number of particles in a way reminiscent of the Schallow-Townes effect.[31]

III. MEAN VALUES

Thanks to the relations $\langle O\rangle = \mathrm{Tr}(O\rho)$ and $\partial_t\langle O\rangle = \mathrm{Tr}(O\partial_t\rho) = \mathrm{Tr}(O\mathcal{L}\rho)$, we can obtain from Eq. (9) the single-time mean values of interest for this problem by solving the equation of motion of the coupled system,

$$\partial_t \begin{pmatrix} n_a \\ n_b \\ n_{ba} \\ n_{ab} \end{pmatrix} = \begin{pmatrix} P_a \\ P_b \\ 0 \\ 0 \end{pmatrix} + \begin{pmatrix} -\Gamma_a & 0 & ig & -ig \\ 0 & -\Gamma_b & -ig & ig \\ ig & -ig & -i\Delta - 2\Gamma_+ & 0 \\ -ig & ig & 0 & i\Delta - 2\Gamma_+ \end{pmatrix} \times \begin{pmatrix} n_a \\ n_b \\ n_{ba} \\ n_{ab} \end{pmatrix}, \tag{12}$$

where $n_c = \langle c^\dagger c \rangle \in \mathbb{R}$ (for $c = a, b$) and $n_{ab} = \langle a^\dagger b \rangle = n_{ba}^* \in \mathbb{C}$. The SE case corresponds to setting $P_{a,b} = 0$ and providing the initial conditions

$$n_a^0 \equiv n_a(0), \quad n_b^0 \equiv n_b(0), \quad \text{and} \quad n_{ab}^0 \equiv n_{ab}(0). \tag{13}$$

The solutions are heavy and are presented elsewhere.[32]

On the other hand, the SS case corresponds to setting the time derivative on the left-hand side of Eq. (12) to zero and solving the resulting set of linear equations. This yields

$$n_a^{\mathrm{SS}} = \frac{g^2\Gamma_+(P_a + P_b) + P_a\Gamma_b\left[\Gamma_+^2 + \left(\frac{\Delta}{2}\right)^2\right]}{4g^2\Gamma_+^2 + \Gamma_a\Gamma_b\left[\Gamma_+^2 + \left(\frac{\Delta}{2}\right)^2\right]}, \tag{14a}$$

$$n_b^{\mathrm{SS}} = \frac{g^2\Gamma_+(P_a + P_b) + P_b\Gamma_a\left(\Gamma_+^2 + \left(\frac{\Delta}{2}\right)^2\right)}{4g^2\Gamma_+^2 + \Gamma_a\Gamma_b\left(\Gamma_+^2 + \left(\frac{\Delta}{2}\right)^2\right)}, \tag{14b}$$

$$n_{ab}^{\mathrm{SS}} = \frac{\frac{g}{2}(\gamma_a P_b - \gamma_b P_a)\left(i\Gamma_+ - \frac{\Delta}{2}\right)}{4g^2\Gamma_+^2 + \Gamma_a\Gamma_b\left[\Gamma_+^2 + \left(\frac{\Delta}{2}\right)^2\right]}. \tag{14c}$$

Both photonic and excitonic reduced density matrices are diagonal. They correspond to thermal distributions of particles with the above mean numbers.[33] Behind their forbidding appearance, Eqs. (14) enjoy a transparent physical meaning, which they inherit from the semiclassical—and therefore intuitive—picture of rate equations. When the coupling strength between the two modes, g, vanishes, the solutions are those of a source and sink problem for bosons

$$n_a^{\mathrm{SS}}(g = 0) = \frac{P_a}{\gamma_a - P_a}, \tag{15}$$

(idem for b throughout by interchanging a and b indexes) i.e., they are solutions of $\partial_t n_a = -\gamma_a n_a + P_a(n_a + 1)$, featuring the famous Bose stimulation effect, whereby the probability of relaxation toward the final state is increased by its population. In the general case where $g \neq 0$, the mean numbers can also be written in the form of Eq. (15),

$$n_a^{\mathrm{SS}} = \frac{P_a^{\mathrm{eff}}}{\gamma_a^{\mathrm{eff}} - P_a^{\mathrm{eff}}}, \tag{16}$$

(idem for $a \leftrightarrow b$), in terms of effective pump and decay rates

$$P_a^{\mathrm{eff}} = P_a + \frac{Q_a}{\Gamma_a + \Gamma_b}(P_a + P_b), \tag{17a}$$

$$\gamma_a^{\mathrm{eff}} = \gamma_a + \frac{Q_a}{\Gamma_a + \Gamma_b}(\gamma_a + \gamma_b), \tag{17b}$$

with Q_a as the rate at which mode a exchanges particles with mode b,

$$Q_a = \frac{4(g^{\mathrm{eff}})^2}{\Gamma_b}, \tag{18}$$

in terms of the effective coupling strength at nonzero detuning,

$$g^{\mathrm{eff}} = \frac{g}{\sqrt{1 + \left(\frac{\Delta/2}{\Gamma_+}\right)^2}}. \tag{19}$$

Q_a is a generalization of the *Purcell rate* $\gamma_a^{\mathrm{P}} = 4g^2/\gamma_b$, which is the rate at which the cavity population decays in weak coupling when $\gamma_b, \gamma_a^{\mathrm{P}} \gg \gamma_a$. From the point of view of mode a, the coupling with mode b is both adding particles, contributing to P_a^{eff}, and removing them, contributing to γ_a^{eff}. The total effective decay is

$$\Gamma_a^{\mathrm{eff}} = \gamma_a^{\mathrm{eff}} - P_a^{\mathrm{eff}} = \Gamma_a + Q_a. \tag{20}$$

Note that the generalized Purcell rate Q_a appears in the same way in both effective parameters in Eq. (17) due to the symmetry of the coupling (which both brings in and removes excitations). The mean value of the coherence can also be expressed in terms of these quantities,

$$n_{ab}^{\mathrm{SS}} = \frac{2g^{\mathrm{eff}}}{\Gamma_a^{\mathrm{eff}} + \Gamma_b^{\mathrm{eff}}} \frac{\gamma_a P_b - \gamma_b P_a}{\Gamma_a \Gamma_b} e^{i\phi}, \tag{21}$$

where $\phi = \arctan\left(\frac{\Gamma_+}{\Delta/2}\right)$.

The quantities defined in Eqs. (17) and (20) are all positive when $\Gamma_b > 0$ ($Q_a > 0$) and all negative when $\Gamma_b < 0$ (if there exists a solution for the steady state). The conditions for the pumping terms P_a, P_b to yield a physical state (a steady state) are therefore those for which the mean values $n_{a,b}^{\mathrm{SS}}$ are positive and finite, implying

$$\Gamma_+ > 0, \tag{22a}$$

$$4(g^{\mathrm{eff}})^2 > -\Gamma_a\Gamma_b. \tag{22b}$$

The first condition requires that pumps P_a, P_b are not *simultaneously* larger than their respective decay rates γ_a, γ_b. The second condition only represents a restriction when one of the effective parameters, either Γ_a or Γ_b, is negative. Then, it reads explicitly $4(g^{\mathrm{eff}})^2 > |\Gamma_a\Gamma_b|$. Note that out of resonance, the pumping rates appear both in g^{eff} and Γ_a, Γ_b, and therefore the explicit range of physical values for them needs to be found self-consistently.

IV. CORRELATION FUNCTIONS AND SPECTRA

We now turn to the main goal of this paper, namely, the luminescence spectrum of the system $s(\omega)$. Physically, it is the mean number of photons in the system with frequency ω, i.e., by definition

$$s(\omega) = \langle a^\dagger(\omega) a(\omega) \rangle. \tag{23}$$

This is proportional to the intensity of photons emitted by the cavity at this frequency [the direct exciton emission from its recombination is described in a similar way by $\langle b^\dagger(\omega) b(\omega) \rangle$]. It will be more convenient, throughout, to deal with normalized spectra,

$$S(\omega) = s(\omega) / \int_0^\infty \langle a^\dagger a \rangle(t) dt, \tag{24}$$

so that Eq. (24) is now the density of probability that a photon emitted by the system has frequency ω. The Fourier transform of $a(\omega)$ relates the emission spectrum to a two-time correlator through $S(\omega) = \frac{1}{2\pi} \int\int_0^\infty \langle a^\dagger(t_1) a(t_2) \rangle \times e^{i\omega(t_2 - t_1)} dt_1 dt_2 / \int_0^\infty \langle a^\dagger a \rangle(t) dt$, which after a change in variables can be expressed in terms of the so-called first-order time autocorrelator,

$$G^{(1)}(t, \tau) = \langle a^\dagger(t) a(t + \tau) \rangle, \tag{25}$$

for positive time delay $\tau = t_2 - t_1 \geq 0$. All put together, this yields the usual Fourier-pair relationship between the power spectrum and the autocorrelation function,

$$S(\omega) = \frac{1}{\pi \int_0^\infty \langle a^\dagger a \rangle(t) dt} \Re \int_0^\infty \int_0^\infty G^{(1)}(t, \tau) e^{i\omega\tau} d\tau dt. \tag{26}$$

Equation (26) holds as such in the SE case. In the SS case, care must be taken with cancellation of infinities brought by the ever-increasing time t. A technical but straightforward procedure[32] leads to the expression that explicitly gets rid of the divergences—famously known as the Wiener-Khintchine theorem[34]—that reads

$$S^{\mathrm{SS}}(\omega) = \frac{1}{\pi} \frac{1}{n_a^{\mathrm{SS}}} \lim_{t \to \infty} \Re \int_0^\infty G^{(1)}(t, \tau) e^{i\omega\tau} d\tau. \tag{27}$$

Possibly, one could use a version of this expression that takes into account experimental details such as the detector linewidth.[35]

From now on, we shall refer with "SE" and "SS" the expressions that apply specifically to the spontaneous emission and to the steady state, respectively, leaving free of index those that are of general validity. In some cases, as for instance in Eq. (10), no index is required if it is understood that $P_{a/b}$ are defined and equal to zero in the SE case. For that reason, we shall leave Γ free of the SE/SS redundant index.

To obtain the spectra of a system whose dynamics is dictated by Eq. (9), we therefore need to compute two-time dynamics. This can be done thanks to the quantum regression theorem, according to which, given a set of operators $C_{\{\eta\}}$ that satisfy $\mathrm{Tr}(C_{\{\eta\}} \mathcal{L} \Omega) = \Sigma_{\{\lambda\}} M_{\{\eta\lambda\}} \mathrm{Tr}(C_{\{\lambda\}} \Omega)$ for any operator Ω (with $M_{\{\eta\lambda\}} \in \mathbb{C}$), the equations of motion for the two-time correlators read

$$\partial_\tau \langle \Omega(t) C_{\{\eta\}}(t + \tau) \rangle = \sum_{\{\lambda\}} M_{\{\eta\lambda\}} \langle \Omega(t) C_{\{\eta\}}(t + \tau) \rangle. \tag{28}$$

In the fully bosonic case, operators $a^m b^n$ with $\{\eta\} = (m, n) \in \mathbb{N}$ constitute such a set with M defined by

$$M_{\substack{mn \\ mn}} = -i(m\omega_a + n\omega_b) - m\frac{\Gamma_a}{2} - n\frac{\Gamma_b}{2}, \tag{29a}$$

$$M_{\substack{mn \\ m+1,n-1}} = M_{\substack{nm \\ n-1,m+1}} = -ign, \tag{29b}$$

and zero everywhere else. For the computation of the optical spectrum, it is enough to consider the set of operators $C = a, b$ and $\Omega = a^\dagger$ in Eq. (28). We obtain the equation

$$\partial_\tau \mathbf{v}(t, t + \tau) = \mathbf{M} \mathbf{v}(t, t + \tau) \tag{30}$$

for the correlators

$$\mathbf{v}(t, t + \tau) = \begin{pmatrix} \langle a^\dagger(t) a(t + \tau) \rangle \\ \langle a^\dagger(t) b(t + \tau) \rangle \end{pmatrix}, \tag{31}$$

where

$$\mathbf{M} = \begin{pmatrix} M_{\substack{10 \\ 10}} & M_{\substack{10 \\ 01}} \\ M_{\substack{01 \\ 10}} & M_{\substack{01 \\ 01}} \end{pmatrix} = \begin{pmatrix} -i\omega_a - \frac{\Gamma_a}{2} & -ig \\ -ig & -i\omega_b - \frac{\Gamma_b}{2} \end{pmatrix}. \tag{32}$$

The formal solution follows straightforwardly from $\mathbf{v}(t, t + \tau) = e^{\mathbf{M}\tau} \mathbf{v}(t, t)$. Made explicit, it reads (at positive τ)

$$\begin{aligned} \langle a^\dagger(t) a(t + \tau) \rangle = \frac{1}{2R} e^{-\Gamma_+ \tau} e^{-i[\omega_a - (\Delta/2)]\tau} \\ \times \{ e^{iR\tau} [(R + i\Gamma_- - \Delta/2) n_a(t) - g n_{ab}(t)] \\ + e^{-iR\tau} [(R - i\Gamma_- + \Delta/2) n_a(t) + g n_{ab}(t)] \} \end{aligned} \tag{33}$$

in terms of the *complex (half) Rabi frequency*

$$R = \sqrt{g^2 - \left(\Gamma_- + i\frac{\Delta}{2} \right)^2}, \tag{34}$$

which arises as a direct extension of the dissipationless case, Eq. (6). For our discussion, it is convenient to decompose R into its real and imaginary parts, $R = R_r + iR_i$. Out of resonance, the Rabi frequency is a complex number with both nonzero real and imaginary parts. On the other hand, at resonance, it is either pure imaginary (in the WC regime) or pure real (in the SC one). For this latter case, it is worth defining a new quantity,

$$R_0 = R(\Delta = 0) = \sqrt{g^2 - \Gamma_-^2}. \tag{35}$$

The real and imaginary parts of R are plotted in Fig. 3 as a function of Γ_- / g for various negative detunings. In the limit of high detuning, $|\Delta| \gg \max(g, \Gamma_-)$, regardless of WC or SC, the real part becomes independent of the dissipation (decay and pumping), $R_r \approx |\Delta| / 2$, and the imaginary part becomes $R_i \approx \mp \Gamma_-$. We can see in Fig. 3 that this sets an upper bound for R_i,

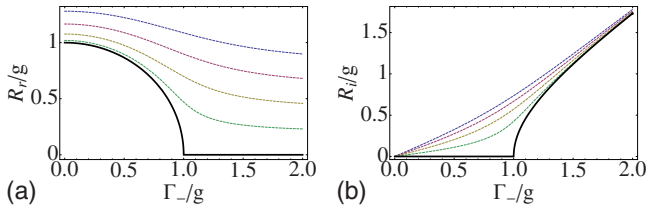

FIG. 3. (Color online) Complex Rabi R/g, separated in its real (a) and imaginary (b) parts, as a function of the decoherence parameter Γ_-/g for various detunings (Δ/g from −1.6, up, to 0, bottom, by steps of 0.4). Solid black lines correspond to resonance.

$$|R_i| < |\Gamma_-|. \tag{36}$$

A physical steady state is obtained for values of P_a, P_b that ensure that the correlator of Eq. (33) converges to zero when $\tau \to \infty$. Here, the condition follows from having a positive total decay rate

$$\Gamma_+ - |R_i| > 0. \tag{37}$$

The first consequence of this condition is simply that Γ_+ must be positive, as we already found with the analysis of the mean values and wrote in Eq. (22a). With $\Gamma_+ > 0$, the other decay rate appearing in Eq. (33) is automatically fulfilled ($\Gamma_+ + |R_i| > 0$). On one hand, if $\Gamma_a, \Gamma_b > 0$, Eq. (37) is always true, as we know that $|R_i| < |\Gamma_-| < \Gamma_+$ [from Eq. (36)]. This includes the spontaneous emission case where there is no restriction in the parameters. On the other hand, if either Γ_a or Γ_b is negative, Eq. (37) represents a further limitation for the pumping parameters. One can check that it is again exactly equivalent to the condition we already found in Eq. (22b). Therefore, the condition that the correlators are well behaved is exactly the same as those that the populations are positive and a physical steady state exists.

Using the result of Eq. (33) into the definition of Eq. (26), we obtain the formal structure of the emission spectrum,

$$S(\omega) = \frac{1}{2}(\mathcal{L}^1 + \mathcal{L}^2) - \frac{1}{2}\Im\{W\}(\mathcal{L}^1 - \mathcal{L}^2) - \frac{1}{2}\Re\{W\}(\mathcal{A}^1 - \mathcal{A}^2), \tag{38}$$

with $\mathcal{L}(\omega)$ and $\mathcal{A}(\omega)$ some Lorentzian and dispersive functions whose features (position and broadening) are entirely specified by the complex Rabi frequency [Eq. (34)], Γ_+ [Eq. (11)], and the detuning Δ,

$$\mathcal{L}^{1,2}(\omega) = \frac{1}{\pi}\frac{\Gamma_+ \pm R_i}{(\Gamma_+ \pm R_i)^2 + \left[\omega - \left(\omega_a - \frac{\Delta}{2} \mp R_r\right)\right]^2}, \tag{39a}$$

$$\mathcal{A}^{1,2}(\omega) = \frac{1}{\pi}\frac{\omega - \left(\omega_a - \frac{\Delta}{2} \mp R_r\right)}{(\Gamma_+ \pm R_i)^2 + \left[\omega - \left(\omega_a - \frac{\Delta}{2} \mp R_r\right)\right]^2}. \tag{39b}$$

We also introduced the weight W, a complex coefficient given by

$$W = \frac{\Gamma_- + i\left(\frac{\Delta}{2} + gD\right)}{R}, \tag{40}$$

which we define in terms of still another parameter, D,

$$D = \frac{\int_0^\infty \langle a^\dagger b\rangle(t)dt}{\int_0^\infty \langle a^\dagger a\rangle(t)dt}. \tag{41}$$

Written in this form, Eqs. (38)–(41) assume a transparent physical meaning with a clear origin for each term. The spectrum consists of two peaks (that we label 1 and 2), as is well known qualitatively for the SC regime. These are composed of a Lorentzian $\mathcal{L}$ and a dispersive $\mathcal{A}$ part. The Lorentzian is the fundamental line shape for a system with a lifetime, and in the expression above, it inherits most of how the dissipation gets distributed in the coupled system, including the so-called *subnatural linewidth averaging* that makes the broadening at resonance below the cavity mode width.[16] The dispersive part originates from the coupling as in the Lorentz (driven) oscillator. In our system, it stems from the driving of one mode by the other because of the coupling. This decomposition of each peak in such terms is therefore clear and expected. The bare cavity mode will be taken as a reference for the energy scales in the rest of the text (we set $\omega_a = 0$).

So far, all the results hold for both cases of SE and SS. This shows that the qualitative depiction of SC is robust. This made it possible to pursue it in a given experimental system with the parameters of the theoretical models fit for another. This has indeed been the situation with semiconductor results explained in terms of the formalism built for atomic systems.

To be complete, the solution now only requires the boundary conditions that are given by the quantum state of the system. They will affect the parameter D, Eq. (41), that is therefore the bridging parameter between the two cases. In the next two sections, we address these two cases and their specificities.

A. Case of spontaneous emission

In the case of spontaneous emission,[16,21] where the system decays from an initial state, the boundary conditions are supplied for $\tau = 0$ by the initial values $\mathbf{v}(t,t)$, i.e., the cavity population, $n_a(t) = \langle a^\dagger a\rangle(t)$ and the coherence element $n_{ab}(t) = \langle a^\dagger b\rangle(t)$. In turn, those are completely defined by the initial conditions, Eqs. (13). Although the analytical expressions for these mean values as a function of time are cumbersome,[32] the D coefficient, Eq. (41), that determines quantitatively the line shape assumes a (relatively) simpler expression,

$$D^{\mathrm{SE}} = \frac{\left[\frac{g}{2}(\gamma_a n_b^0 - \gamma_b n_a^0) - 2in_{ab}^0(\gamma_+^2 - \gamma_-^2)\right]\left(i\gamma_+ - \frac{\Delta}{2}\right) + 2g^2\gamma_+ \Re n_{ab}^0}{g^2\gamma_+(n_a^0 + n_b^0) + n_a^0\gamma_b\left[\gamma_+^2 + \left(\frac{\Delta}{2}\right)^2\right] + g\gamma_b\left(\frac{\Delta}{2}\Re n_{ab}^0 + \gamma_+ \Im n_{ab}^0\right)}. \tag{42}$$

To prepare the analogy with the SS case in the next section, we also write the particular case when $n_{ab}^0 = 0$,

$$D^{\mathrm{SE}} = \frac{\frac{g}{2}(\gamma_a n_b^0 - \gamma_b n_a^0)\left(i\gamma_+ - \frac{\Delta}{2}\right)}{g^2\gamma_+(n_a^0 + n_b^0) + n_a^0\gamma_b\left[\gamma_+^2 + \left(\frac{\Delta}{2}\right)^2\right]}. \tag{43}$$

This is an important case as it is realized whenever the initial population of one of the modes is zero, which is the typical experimental situation. Note that in this case, D^{SE}, and therefore also the normalized spectra, does not depend on the two populations independently but on their ratio only,

$$\alpha = \frac{n_a^0}{n_b^0}. \tag{44}$$

B. Case of continuous incoherent pumping

In the case where the system is excited by a continuous incoherent pumping, a steady state is reached and the boundary conditions are given by the stationary limit, as time tends to infinity, of the dynamical equation (whose solution is unique). The D parameter, Eq. (41), is defined in this case as

$$D^{\mathrm{SS}} = \frac{n_{ab}^{\mathrm{SS}}}{n_a^{\mathrm{SS}}} = \frac{\frac{g}{2}(\gamma_a P_b - \gamma_b P_a)\left(i\Gamma_+ - \frac{\Delta}{2}\right)}{g^2\Gamma_+(P_a + P_b) + P_a\Gamma_b\left[\Gamma_+^2 + \left(\frac{\Delta}{2}\right)^2\right]}. \tag{45}$$

There is a clear analogy between Eq. (45)—that corresponds to the SS—and Eq. (43)—that corresponds to SE when $n_{ab}^0 = 0$. In this case, the spectrum can also be written in terms of the ratio, counterpart of Eq. (44),

TABLE I. Expression of D, Eq. (41), as a function of α, Eqs. (44) and (46), in the SE (with $\Gamma_{\pm,a,b} \to \gamma_{\pm,a,b}$ and $n_{ab}^0 = 0$) and SS cases. D embodies in the luminescence spectrum the influence of the quantum state of the system. The latter is specified by the initial condition in SE or the pumping/decay interplay in the SS.

$\alpha = \frac{n_a^0}{n_b^0} = \frac{P_a}{P_b}$	D
0	$\frac{-\frac{g}{2}\left(i\Gamma_+ - \frac{\Delta}{2}\right)\gamma_b}{g^2\Gamma_+ + \Gamma_b\left[\Gamma_+^2 + \left(\frac{\Delta}{2}\right)^2\right]}$
$0 < \alpha < \infty$	$\frac{\frac{g}{2}\left(i\Gamma_+ - \frac{\Delta}{2}\right)(\gamma_a - \gamma_b\alpha)}{g^2\Gamma_+(1+\alpha) + \alpha\Gamma_b\left[\Gamma_+^2 + \left(\frac{\Delta}{2}\right)^2\right]}$
∞	$\frac{\left(i\Gamma_+ - \frac{\Delta}{2}\right)\gamma_a}{2g\Gamma_+}$

$$\alpha = \frac{P_a}{P_b}, \tag{46}$$

in which case Eqs. (43) and (45) assume the same expression, keeping in mind the definition of Eqs. (10). Table I displays this common expression of D in terms of α. The limiting cases when $\alpha \to 0$ or ∞ are also given. They correspond to only photons or excitons as the initial state for the SE or to the presence of only one kind of incoherent pumping for the SS case.

The analogy and differences between D^{SE} and D^{SS} reflect in the spectra S^{SE} and S^{SS}. For the same α, they become identical when the pumping rates are negligible as compared to the decays, $P_{a,b} \ll \gamma_{a,b}$. In this case, where $\Gamma_{\pm,a,b} \approx \gamma_{\pm,a,b}$, the SS system indeed behaves similar to that of the SE of particles that decay independently and that are, at each emission, either a photon or an exciton, with probabilities in the ratio α.

However, in the most general case, D^{SS} depends on more parameters than D^{SE}. Moreover, the pumping rates $P_{a,b}$ affect S^{SS} not only through α and D^{SS} but also in the position and broadening of the peaks (given by $\Gamma_\pm$ and R). Therefore, the SS is a more general case, from which the SE with $n_{ab}^0 = 0$ can be obtained, but not the other way around. On the other hand, as seen in Table I, the SS case cannot recover the SE case when $n_{ab}^0 \neq 0$. Further similarities could be found if cross Lindblad pumping terms were introduced in Eq. (9) with parameters P_{ab} in analogy to the cross initial mean value n_{ab}^0, as done in, e.g., Ref. 36, but this describes a different system where polaritons can also be directly excited. In the present one, none of the SE and SS cases comprises all the possibilities of the other. Anyhow, an important fact for the semiconductor community is that a SS with nonvanishing pumping rates is out of reach of the SE of any initial state, which has been the case studied in the literature so far,[16,21] and that even in this limiting case, the effective quantum state obtained in the SS should still be resolved self-consistently, rather than assuming for α the particular case 0 or ∞.

C. Discussion

With this exposition of the analytical expressions of the luminescence spectra, and the discussion of their similarity and distinctions that we have just given, the coverage of the problem is complete. In order to give a more physical picture of these abstract results, we shall in the rest of this paper illustrate the implications that this bears in practical terms. We consider the case of resonance for this purpose, for reasons detailed in the next section. This will also allow us to provide self-contained expressions for the spectra. Detuning is however important for a nonlinear fitting of the experi-

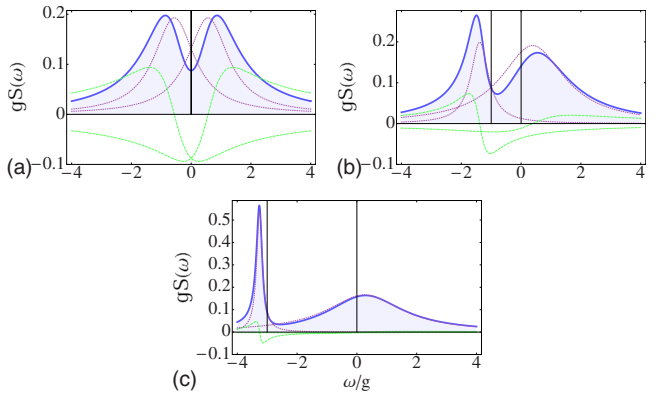

FIG. 4. (Color online) Strong-coupling steady-state spectra (blue solid line) and their decomposition into Lorentzian (dotted purple) and dispersive parts (dashed green) for various detunings ($\Delta/g=0,1,3$) with parameters of point (c) of Fig. 8: $\gamma_a=3.8g$, $\gamma_b=0.1g$, $P_a=0.5g$, $P_b=0.1g$. The vertical black lines mark the positions of the bare modes (cavity at $\omega_a=0$ and exciton at $\omega_b=-\Delta$), showing the "level repulsion" of SC.

mental data.[37–47] The system lends itself naturally to a global fitting of such data, i.e., constraining all fitting parameters over the various detuning cases, where only the detuning is allowed to vary, while optimizing them globally.[48] This procedure provided excellent agreement between our theoretical model and the experimental data in Ref. 37 and extending this practice could tell much about which microscopic details and/or which physical model rule a particular structure.[49]

There is no difficulty in extending all the discussions that follow to arbitrary detunings. For instance, Fig. 4 shows the SS spectra and their mathematical decompositions into Lorentzian and dispersive parts, as detuning is varied. Figures 4(b) and 4(c) are obtained using Eqs. (38)–(41), and in this particular case, expression (45) for D. Figure 4(a), the case at resonance, can be obtained in the same way, but in next section we shall bring all these results together in a condensed expression when $\Delta=0$ [Eq. (58)].

More importantly, as we shall soon appreciate, the resonant case is the pillar of the SC physics. The main output of the out-of-resonance case is to help identify or to characterize the resonance, for instance, by localizing it in an anticrossing or by providing useful additional constrains with only one more free parameter in a global fitting. Even a slight detuning brings features of WC into the SC system and ultimately, when $|\Delta| \gg g$, the complex Rabi frequency converges into the same expression for both regimes (as shown in Fig. 3). This is why we now consider the SC problem in its purest form: when the coupling between the modes is optimum.

V. STRONG AND WEAK COUPLING AT RESONANCE

Strong coupling is most marked at resonance, and this is where its signature is experimentally ascertained, in the form of an anticrossing. Fundamentally, there is another reason why resonance stands out as predominant; this is where a criterion for SC can be defined unambiguously in presence of dissipation.

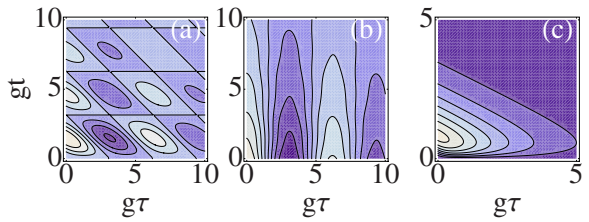

FIG. 5. (Color online) Time dynamics of the correlator $\Re\langle a^\dagger(t)a(t+\tau)\rangle^{\mathrm{SE}}$, cf. Eq. (33). Only the pattern of oscillations is of interest here (lighter blues correspond to higher values). In all cases, both the t and τ dynamics tend to zero. Figures (a) and (b) show the SE of an exciton and of an upper polariton, respectively, in a very strongly coupled system ($\gamma_a=0.2g$ and $\gamma_b=0.1g$). Figure (c) shows the SE of an exciton in weak coupling ($\gamma_a=5.9g$). The oscillations in τ, rather than in t, are the mark of strong coupling.

WC and SC are formally defined as the regime where the complex Rabi frequency at resonance, Eq. (35), is pure imaginary (WC) or real (SC).

This definition, which takes into account dissipation and pumping, generalizes the classification found in the literature. The reason for this definition is mainly to be found in the behavior of the time autocorrelator, Eq. (33), that is, respectively, damped or oscillatory as a result. The exponential damping is the usual manifestation of dissipation, which decays the correlations in the field, even when a steady state is maintained. On the other hand, in the same situation of steady averages (no dynamics) but now in SC, oscillations with τ are the mark of a coherent exchange between the bare fields (photon and exciton).

In the literature, one sometimes encounters the confusion that SC is linked to a periodic transfer of energy or of population between the photon and exciton field, or that it follows from a chain of emissions and absorptions. This is an incorrect general association as one can exhibit explicit cases with apparent oscillations of populations that correspond to weak coupling, or on the contrary, cases with no oscillations of populations that are in SC. The two concepts are therefore unrelated in the sense that none implies the other. This is illustrated for the SE case in Figs. 5(a), 5(b), and 6 on one hand, where the system is in SC, and in Fig. 5(c) on the other hand, where it is in WC. In SS, there is no t dynamics in any case, so oscillations of populations are clearly unrelated to weak or strong coupling. In SE, the distinction is clearly seen

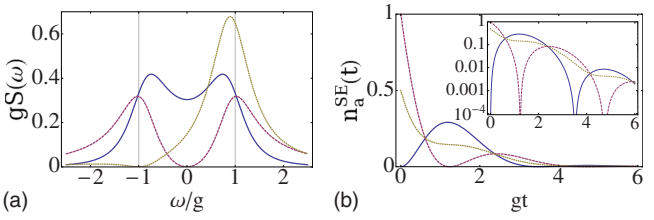

FIG. 6. (Color online) (a) Strong-coupling spectra $S_0^{\mathrm{SE}}(\omega)$ and (b) its corresponding mean number dynamics $n_a^{\mathrm{SE}}(t)$ for the spontaneous emission of three different initial states. In blue solid, one exciton; in purple dashed, one photon; and in brown dotted, one upper polariton. Parameters are $\gamma_a=1.9g$ and $\gamma_b=0.1g$. Inset of (b) is the same in log scale.

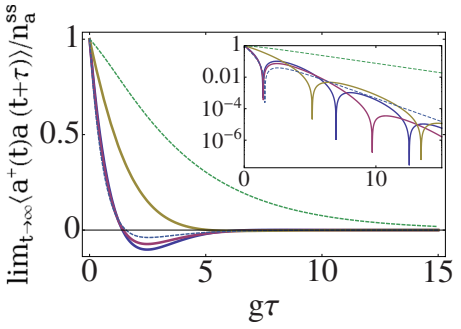

FIG. 7. (Color online) Dynamics of $\lim_{t\to\infty}\langle a^\dagger(t)a(t+\tau)\rangle/n_a^{SS}$, Eqs. (14a) and (33), for the steady state corresponding to points (a)–(e) in Fig. 8. In the inset, the same in log scale. Solid lines [(b) blue, (c) purple, and (d) brown] of SC feature oscillations of the correlator, as the mark of SC. Dashed lines [(a) green and (e) blue] correspond to weak coupling. Note that although the blue dashed line (e) appears to be similar to other SC lines, it does not oscillate in the log scale, where it only features a single local minimum. In the same way, the brown line (d) that seems not to oscillate actually features an infinite set of local minima, as is revealed in the log scale.

in Fig. 5 where both the t and τ dynamics are shown in a contour plot in the case where the system is initially prepared as an exciton, (a) and (c), or as a polariton, (b). In the polariton case, the dynamics in t is simply decaying (because of the lifetime), while it is clearly oscillating in τ, where the proper manifestation of SC is to be found. The t decay is not exactly exponential because in the presence of dissipation, the polariton is not an ideal eigenstate anymore (the larger the dissipation, the more the departure). However this effect in SC is so small that it only consists of a small "wobbling" of the τ contour lines. On the other hand, the exciton, (a), that is not an eigenstate features oscillations both in the t dynamics (the one often but unduly regarded as the signature of SC), as well as the τ dynamics. In stark contrast, the exciton in WC, (c), bounces with t. This, that might appear as an oscillation, is not as it happens only once and is damped at long times. This behavior is shown quantitatively in Fig. 6 for SC, where the population $n_a(t)$ is displayed for the SE of an exciton (blue solid), a photon (purple dashed) and an upper polariton (brown dotted), respectively, along with the luminescence spectrum that they produce (detected in the cavity emission). Here it is better seen how, for instance, the polariton decay is wobbling as a result of the dissipation that perturbs its eigenstate character and leaks some population to the lower polariton. More importantly, note how very different the spectra are, depending on whether the initial state is a photon or an exciton, despite the fact that the dynamics is similar in both cases (see the inset in log scale of their respective populations). The PL spectrum observed in the cavity emission is much better resolved when the system is initially in a photon state than it is when the system is initially in an exciton state. The splitting is larger and the overlap of the peaks smaller in the former case. This will find an important counterpart in the SS case.

Figure 7 shows the τ dynamics in the SS (when the t dynamics has converged and is steady) for five cases of interest to be discussed later (in Fig. 8). A first look at the dynamics would seem to gather together a group of two curves that decay exponentially to good approximation (and remain positive as a result) and another group of three that assume a local minimum. The correct classification is the most counterintuitive in this regard, as it puts together the dashed lines on one hand and the solid on the other. The mathematical reason for this classification is revealed in the inset, where the same dynamics is plotted in log scale. The dashed (solid) lines correspond to parameters where the system is in WC (SC) according to the definition, i.e., to values of R that are imaginary on one hand and real on the other. In log scale, this corresponds, respectively, to a damping of the correlator, against oscillations with an infinite number of local minima. Note that the blue dashed line features one local minimum, which does not correspond to an oscillatory—or coherent-exchange—behavior of the fields but rather to a jolt in the damping. These considerations that may appear abstract at this level will later turn out to show up as the actual emergence, or not, of the split (dressed) states.

We now return to the general (SE/SS) expression for the spectra, Eq. (38), that, at resonance in SC, simplifies to

$$S_0(\omega) = \frac{1}{2}(\mathcal{L}_s^1 + \mathcal{L}_s^2) - \frac{g\Re\{D_0\}}{2R_0}(\mathcal{L}_s^1 - \mathcal{L}_s^2) + \frac{g\Im\{D_0\} - \Gamma_-}{2R_0}(\mathcal{A}_s^1 - \mathcal{A}_s^1), \tag{47}$$

where we used the definition for the (half) Rabi frequency at resonance, Eq. (35), and

$$\mathcal{L}_s^{1,2}(\omega) = \frac{1}{\pi}\frac{\Gamma_+}{\Gamma_+^2 + (\omega \pm R_0)^2}, \tag{48a}$$

$$\mathcal{A}_s^{1,2}(\omega) = \frac{1}{\pi}\frac{\omega \pm R_0}{\Gamma_+^2 + (\omega \pm R_0)^2}. \tag{48b}$$

In the weak-coupling regime, with R_0 being pure imaginary ($g < |\Gamma_-|$), the positions of the two peaks collapse onto the center, $\omega_a = \omega_b = 0$. Defining $iR_w = R_0$, with $R_w = \sqrt{\Gamma_-^2 - g^2}$ being a real number, the general expression for the spectra rewrites as

$$S_0^w(\omega) = \left(\frac{1}{2} + \frac{\Gamma_- - g\Im\{D_0\}}{2R_w}\right)\mathcal{L}_w^1 + \left(\frac{1}{2} - \frac{\Gamma_- - g\Im\{D_0\}}{2R_w}\right)\mathcal{L}_w^2 - \frac{g\Re\{D_0\}}{2R_w}(\mathcal{A}_w^1 - \mathcal{A}_w^2), \tag{49}$$

with the Lorentzian and dispersive contributions now given by

$$\mathcal{L}_w^{1,2}(\omega) = \frac{1}{\pi}\frac{\Gamma_+ \pm R_w}{(\Gamma_+ \pm R_w)^2 + \omega^2}, \tag{50a}$$

$$\mathcal{A}_w^{1,2}(\omega) = \frac{1}{\pi}\frac{\omega}{(\Gamma_+ \pm R_w)^2 + \omega^2}. \tag{50b}$$

Before addressing the specifics of the SE and SS cases, it is important to note that at resonance, the Lorentzian and dispersive parts [Eqs. (48) and (50)] are invariant under the

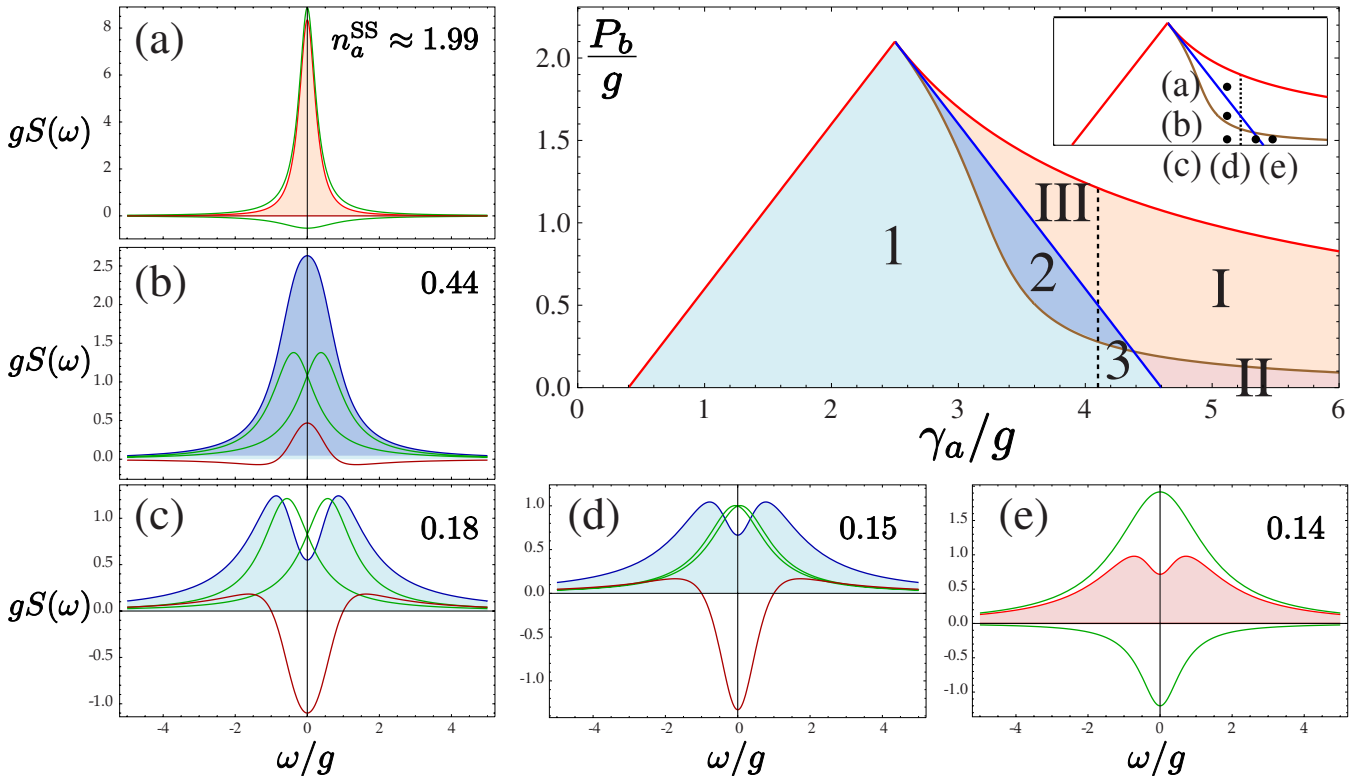

FIG. 8. (Color online) Phase space of the steady-state strong/weak coupling as a function of P_b/g and γ_a/g for the parameters $\gamma_b=0.1g$ and $P_a=0.5g$. The red lines delimit the region where there is a steady state [Eqs. (62) and (63)]. The blue line, Eq. (64), separates the strong (in shades of blue) from the weak (shades of red) coupling regions. The dotted black line, Eq. (65), separates SC and WC regions in the absence of pumping. The brown line, Eq. (66), separates the regions where one (dark blue) or two (light blue) peaks can be resolved in the luminescence spectra. This defines three areas in the SC region: (1) two peaks are resolved in the spectra, (2) the two peaks cannot be resolved and effectively merge into one, albeit in SC, and (3) SC is achieved thanks to the pump P_a (with one or two peaks visible depending of the overlap with the light or dark area) despite the large dissipation that predicts WC according to Eq. (59). In the same way we can distinguish three regions in weak coupling: (I) standard WC, (II) SC with a two peaked spectrum, and (III) WC due to pumping P_b. The surrounding figures (a)–(e) show spectra (filled) from these regions and their decomposition into Lorentzian (green) and dispersive (brown) parts. Parameters correspond to the points in the inset: (a) $\gamma_a=3.8g$ and $P_b=g$, (b) $\gamma_a=3.8g$ and $P_b=0.5g$, (c) $\gamma_a=3.8g$ and $P_b=0.1g$, (d) $\gamma_a=4.49g$ and $P_b=0.1g$, (e) $\gamma_a=4.8g$ and $P_b=0.1g$. Observe how, in SC, two eigenstates have emerged, even in the cases—like in (b)—where they are not seen in the total spectrum. In the same way, in WC, all the emission emanates from the origin, although a two-peak structure can arise as a result of a resonance, also centered at the origin.

exchange of indexes $a \leftrightarrow b$. Therefore, the photon and the exciton spectrum are composed of the same line shapes differing in the prefactor that weighs them in Eq. (47).

A. Case of spontaneous emission

In the most general case of SE, the D^{SE} coefficient at resonance, D_0^{SE}, is a complex number. If the initial condition further fulfils $\Re n_{ab}^0=0$, it becomes pure imaginary. Usually, the initial states considered are independent states of photons or excitons (not a quantum superposition), where indeed $n_{ab}^0=0$.[16,21] In these cases,

$$D_0^{SE} = i\frac{\frac{g}{2}(\gamma_a n_b^0 - \gamma_b n_a^0)}{g^2(n_a^0+n_b^0)+n_a^0\gamma_b\gamma_+}, \tag{51}$$

which yields the following expression for the spectrum:

$$S_0^{SE}(\omega) = \frac{1}{\pi}\frac{\frac{\gamma_a+\gamma_b}{2}\left(g^2+\frac{\gamma_a\gamma_b}{4}\right)\left(g^2 n_b^0+\frac{n_a^0\gamma_b^2}{4}+n_a^0\omega^2\right)}{\left[\omega^4+\omega^2\left(\frac{\gamma_a^2+\gamma_b^2}{4}-2g^2\right)+\left(g^2+\frac{\gamma_a\gamma_b}{4}\right)^2\right]\left[g^2(n_a^0+n_b^0)+n_a^0\gamma_b\frac{\gamma_a+\gamma_b}{4}\right]}. \tag{52}$$

The SE spectrum of exciton observed in the leaky modes is obtained from Eq. (52) by exchanging the indexes $a \leftrightarrow b$. We illustrate this with the two particular cases that follow.

The typical detection geometry for the spontaneous emission of an atom in a cavity consists in having the atom in its excited state as the initial condition and observing its direct emission spectrum. In this case the role of the cavity is merely to affect the dynamics of its relaxation that is oscillatory with the light field in the case of SC. This case corresponds to $n_b^0=1$ and $n_a^0=n_{ab}^0=0$ in Eq. (52) with $a \leftrightarrow b$. This gives[16]

$$S_0^{\mathrm{SE}}(\omega) = \frac{1}{\pi} \frac{\frac{\gamma_a+\gamma_b}{2}\left(g^2+\frac{\gamma_a\gamma_b}{4}\right)\left(\frac{\gamma_a^2}{4}+\omega^2\right)}{\omega^4+\omega^2\left(\frac{\gamma_a^2+\gamma_b^2}{4}-2g^2\right)+\left(g^2+\gamma_a\frac{\gamma_a+\gamma_b}{4}\right)\left(g^2+\frac{\gamma_a\gamma_b}{4}\right)^2}. \tag{53}$$

In the semiconductor case, one would typically still have in mind the excited state of the exciton as the initial condition, but this time, this is the cavity emission that is probed. The initial condition is therefore the same as before but without interchanging a and b in Eq. (52), which reads in this case

$$S_0^{\mathrm{SE}}(\omega) = \frac{1}{\pi} \frac{2(\gamma_a+\gamma_b)(4g^2+\gamma_a\gamma_b)}{16\omega^4-4\omega^2(8g^2-\gamma_a^2-\gamma_b^2)+(4g^2+\gamma_a\gamma_b)^2}. \tag{54}$$

The difference in the line shape due to the initial quantum state is seen in Fig. 6. The visibility of the line splitting is much reduced in the case of an exciton in SC which SE is detected through the cavity emission than in the case of a photon. With a polariton as an initial state, only one line is produced.

Again, by symmetry, interchanging $a \leftrightarrow b$ in Eqs. (53) and (54) corresponds to the SE of the system prepared as a photon at the initial time and detected in, respectively, the cavity emission on one hand [Eq. (53), $a \leftrightarrow b$], and in the leaky mode emission on the other hand [Eq. (54)]. In the latter case, the spectrum is invariant under the exchange $a \leftrightarrow b$. Figure 6 also hints to the changes brought by the detection channel (direct emission of the exciton or through the cavity mode).

If $n_a^0=0$ or $n_b^0=0$ (in which case $n_{ab}^0=0$), the normalized spectra do not depend on the nonzero value n_b^0 or n_a^0. That is, one cannot distinguish in the line shape the decay of one exciton from that of two, or more. In the more general case, when $n_{ab}^0 \neq 0$, the peaks can be differently weighted. For instance, starting with an upper polariton $|U\rangle=(|1,0\rangle+|0,1\rangle)/\sqrt{2}$ ($n_a^0=n_b^0=n_{ab}^0=1/2$) gives rise to a dominant upper-polariton peak (labeled 2 in the above equations, as seen in the brown dotted line in Fig. 6). One can classify the possible line shapes obtained for various initial states. For instance, as we have just mentioned, the normalized spectrum of $|0,n\rangle$ as an initial state is the same whatever the nonzero n, which is not unexpected from a linear model. From the previous statement, the same spectrum is also obtained for a coherent state or a thermal state of photons, or indeed any quantum state, as long as the exciton population remains zero. In the same way, the PL spectrum of the product of coherent states in the photon and exciton fields, $|z\rangle|z'\rangle$ with $z=z' \in \mathbb{C}^*$, is the same as that of a polariton state $|U\rangle$, although both are very different in character: a classical state on one hand and a maximally entangled quantum state on the other.

B. Case of continuous incoherent pumping

In the SS, at resonance, D_0^{SS} is pure imaginary,

$$D_0^{\mathrm{SS}} = i\frac{\frac{g}{2}(\gamma_a P_b - \gamma_b P_a)}{g^2(P_a+P_b)+P_a\Gamma_b\Gamma_+}, \tag{55}$$

and the term that consists in the difference of Lorentzians in Eq. (38) disappears, $\Im\{W\}=0$. As a result, the two peaks are equally weighted for any combination of parameters,

$$S_0^{\mathrm{SS}}(\omega) = \frac{1}{2}(\mathcal{L}_s^1+\mathcal{L}_s^2) + \frac{g\Im\{D_0^{\mathrm{SS}}\}-\Gamma_-}{2R_0}(\mathcal{A}_s^1-\mathcal{A}_s^2). \tag{56}$$

The only way to weigh one of the peaks more than the other in the SS of an incoherent pumping would be to pump directly the polariton (dressed) states, as the case in higher-dimensional systems where polariton states with nonzero momentum relax into the ground state[50] or in the 0D case when cross pumping is considered.[36] In the present model, however, such terms are excluded. The two peaks of the Rabi doublet, composed of a Lorentzian and a dispersive part, are both symmetric with respect to $\omega_a=\omega_b=0$. Only if $\Im\{D_0^{\mathrm{SS}}\}=\Gamma_-/g$, the spectrum of Eq. (56) consists exclusively of two Lorentzians. The parameters that correspond to this case are those fulfilling either $g^2=\frac{P_a}{P_b-P_a}\Gamma_b\Gamma_-$ or $\Gamma_+=0$. The second case corresponds to the limiting case of diverging populations, where the SC becomes arbitrarily good. Note that these spectra, composed of Lorentzians only, are the same in the exciton or photon channel of emission due to the invariance under the exchange $a \leftrightarrow b$. In the most general case, the dispersive part has a small quantitative contribution, bringing closer or further apart the maxima and thus altering the apparent magnitude of the Rabi splitting. In some cases, as we shall discuss, it can however contrive to blur the resolution of the two peaks. A single peak is then observed even though the modes split in energy. As for the weak-coupling formula, it simplifies to

$$S_0^w(\omega) = \left(\frac{1}{2}+\frac{\Gamma_- - g\Im\{D_0\}}{2R_w}\right)\mathcal{L}_w^1 + \left(\frac{1}{2}-\frac{\Gamma_- - g\Im\{D_0\}}{2R_w}\right)\mathcal{L}_w^2, \tag{57}$$

losing completely the dispersive contribution. Both decompositions, Eqs. (56) and (57), have been given to spell out the structure of the spectra in both regimes. The unified expression that covers them both reads explicitly

$$S_0^{\mathrm{SS}}(\omega) = \frac{1}{\pi n_a^{\mathrm{SS}}} \frac{8g^2P_b+2P_a(4\omega^2+\Gamma_b^2)}{16\omega^4-4\omega^2(8g^2-\Gamma_a^2-\Gamma_b^2)+(4g^2+\Gamma_a\Gamma_b)^2}. \tag{58}$$

It is the counterpart for SS of Eq. (52), for SE. The case of excitonic emission can also be obtained, as for SE, exchanging the indexes $a \leftrightarrow b$.

C. Discussion

The spectra in the semiconductor case that are probed at negligible electronic pumping ($P_b \ll 1$) with no cavity pumping ($P_a=0$) are in principle described by the same expression as that of the SE case used in the atomic model. In practice, however, both of these conditions can be easily violated. The renormalization of γ_b with P_b brings significant corrections well in the regime where n_a, $n_b \ll 1$, and one could think that the pump is negligible. For instance, for parameters of point (c) in Fig. 8 with $P_a=0$, the rate P_b that is needed to bring a 100% correction to γ_b yields, according to Eqs. (14a) and (14b), average populations much below unity, namely, $n_a^{SS} \approx 0.026$ and $n_b^{SS} \approx 0.121$. By the time n_b reaches unity, with n_a still one fourth smaller, the correction on the effective decay rate has became 400%. Because of thermal fluctuations in the particle numbers, for these average values, the results are already irreconcilable with a SE emission case. They are, as we shall see in part II of this work,[13] also irreconcilable with a fermion model. As this is n_a which is proportional to the signal detected in the laboratory, the electronic pumping must be kept very small so that corrections to the effective linewidth can be safely neglected. As regimes with high occupation numbers are reached, the renormalized Γs become very different from the bare γs in this model.

Second, even in the vanishing electronic pumping limit, it must be held true that P_a is zero. Even if only an electronic pumping is supplied externally by the experiment, the pumping rates of the model are the effective excitation rates of the cavity and exciton field inside the cavity, and it is clear that photons get injected in the cavity in structures that consists of numerous spectator dots surrounding the one in SC (cf. Fig. 2). Although most of these dots are in WC and out of resonance with the cavity, they affect the dynamics of the SC QD by pouring cavity photons in the system. In the steady state, following our previous discussion, this corresponds to changing the effective quantum state for the emission of the strongly coupled QD. As we shall see in more detail in what follows, this bears huge consequences on the appearance of the emitted doublet, especially on its visibility.

To fully appreciate the importance and deep consequences of these two provisions made by the SS case on its SE counterpart, we devote the rest of this section to a vivid representation in the space of pumping and decay rates. Now that it has been made clear what the relationship between the SE and the SS cases is, we shall focus on the latter that is the adequate general formalism to describe SC of QDs in microcavities.

In presence of a continuous incoherent pumping, the criterion for SC—from the requirement of energy splitting and oscillations in the τ dynamics that we have discussed above—gets upgraded from its usual expression[16]

$$g > |\gamma_-| \tag{59}$$

to the more general condition

$$g > |\Gamma_-|. \tag{60}$$

The quantitative and qualitative implications and their extent are shown in Fig. 8, where we have fixed the parameters $\gamma_b=0.1g$ and $P_a=0.5g$, and outlined the various regions of interest as P_b and γ_a are varied (central panel). This choice of representation allows us to investigate configurations that can be easily imprinted experimentally in the system—by tuning P_b in cavities that have different quality factors (inversely proportional to γ_a).

The red lines enclosing the filled regions in the central plot, delimit a frontier above which the pump is so high that populations diverge (there is no steady state). This is given by the equivalent conditions that we derived in two different ways, Eqs. (22) and (37). At resonance, they simplify to

$$\Gamma_+ > 0, \tag{61a}$$

$$4g^2 > -\Gamma_a \Gamma_b. \tag{61b}$$

In the SC regime, the first condition is sufficient, $R_i=0$, and the total decay rate for the system is given only by Γ_+ [condition (61b) is therefore automatically fulfilled]. The equation for the border of the physical region in SC reads

$$P_b = \gamma_a + \gamma_b - P_a \quad \text{(boundary of SC)}. \tag{62}$$

In the WC regime, condition (61b) becomes restrictive and the limiting value for P_b reads

$$P_b = \gamma_b + Q_b = \gamma_b + \frac{4g^2}{\gamma_a - P_a} \quad \text{(boundary of WC)}, \tag{63}$$

and can be interpreted as the point where the effective decay rate for mode b (direct losses plus its Purcell emission through mode a) is exactly counterbalanced by the effective pump [$\Gamma_b^{\text{eff}}=0$, from Eq. (20)].

The main separation inside that region where a SS exists is between SC (in shades of blue, inside the triangle) and WC (in shades of red, on its right elbow). The blue solid line that marks this boundary is specified by $g=|\Gamma_-|$, i.e., by

$$P_b = 4g - \gamma_a + \gamma_b + P_a \quad \text{(SS transition between SC and WC)}. \tag{64}$$

The dashed vertical black line, specified by $g=|\gamma_-|$, i.e., by

$$\gamma_a = 4g + \gamma_b \quad \text{(SE transition between SC and WC)}, \tag{65}$$

corresponds to the standard criterion of SC (without incoherent pumping).

The light-blue region, labeled 1 in Fig. 8, corresponds to SC as it is generally understood. The luminescence spectrum shows a clear splitting of the lines. The dark-blue region, labeled 2, corresponds to SC, according to the requisite that R_0 must be real, but with a broadening of the lines so large that in the luminescence spectrum, Eq. (56), only one peak is resolved. This region is delimited by the brown line, which is the solution of the equation $d^2S(\omega)/d\omega^2|_{\omega=0}=0$, i.e., no concavity of the spectral line at the origin. From this condition follows the implicit equation

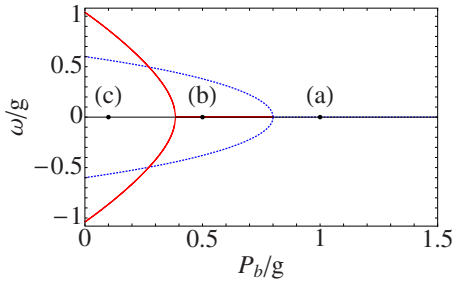

FIG. 9. (Color online) Rabi splitting at resonance (dotted blue) given by $\pm\Re(R_0)$, Eq. (35), and the observed position of the peaks in the PL spectra (solid red) as a function of P_b/g. Parameters are those of the line of points (a)–(c) of Fig. 8: $\gamma_a=3.8g$, $\gamma_b=0.1g$, $P_a=0.5g$. The corresponding P_b are marked for those points.

$$(3\Gamma_+ - \Gamma_-)g^2 + (\Gamma_- - \Gamma_+)^3 + g|D_0|(g^2 - \Gamma_-^2 + 3\Gamma_+^2) = 0 \tag{66}$$

that yields two solutions, only one of which is physical. The other one is placed on the red line $\Gamma_+=0$, where the system diverges and the Rabi peaks become delta functions $\delta(\omega \pm g)$. Note that this line extends into the WC region, as we shall discuss promptly. The distinction between line splitting, as it results from the emergence of new dressed states in the SC, and the observation of two peaks in the spectrum, is seen clearly in Fig. 9, where the two are superimposed and seen to differ greatly even at a qualitative level for most of the range of parameters, coinciding only in a narrow region. The doublet, as observed in the luminescence spectrum, collapses much before SC is lost. Any estimation of system parameters, such as the coupling strength, from a naive interpretation of the peak separation in the PL spectrum will most likely be off by a large amount.

The last region of SC, labeled 3, is that specified by $4g + \gamma_b < \gamma_a < 4g + \gamma_b + P_a - P_b$, i.e., that which satisfies Eq. (60) but violates Eq. (59), thereby being in SC according to the more general definition that takes into account the effect of the incoherent pumping but, according to the conventional criterion, is in WC. For this reason, we refer to this region as of *pump-aided strong coupling*. This is a region of strong qualitative modification of the system that should be in WC according to the intrinsic system parameters (γ_a, γ_b, g) but restores SC thanks to the cavity photons forced into the system.

We now consider the other side of the blue line that displays the counterpart behavior in the WC. Region I is that of WC in its most natural expression. Region II, in light, is the extension into WC of featuring two maxima in the emission spectrum. In this case, this does not correspond to a line splitting in the sense of SC where each peak is assigned to a renormalized (dressed) state, but rather to a resonance of the Fano type that is carving a hole in the single line of the weakly coupled system. In this region, one needs to be cautious not to read SC after the presence of two peaks at resonance. Finally, region III is the counterpart of region 3 in the sense that, according to the conventional criterion for the system parameters [Eq. (59)], this region should be in SC when in reality the too-high electronic pumping has bleached it.

In the inset of Fig. 8, central panel, we reproduce the diagram to position the five points (a)–(e) in the various regions discussed, for which the luminescence spectra are displayed and decomposed into their Lorentzian (green lines) and dispersive (brown) contributions, Eqs. (48) and (50). Case (c), at the lower-left angle, corresponds to SC without any pathology nor surprise; the doublet in the luminescence spectrum—although displaced in position as shown in Fig. 9—is a faithful representation of the underlying Rabi splitting. Increasing pumping brings the system into region 2 where, albeit still in SC, it does not feature a doublet anymore. The reason why is clear on the corresponding decomposition of the spectrum, Fig. 8(b), with a broadening of the dressed states (in green) too large as compared to their splitting. Further increasing the pump brings it out of the SC region to reach point (a), where the two Lorentzians have collapsed on top of each other. This degeneracy of the mode emission means that the coupling only affects perturbatively each mode. As a result, the dispersive correction has vanished, and the spectrum now decomposes into two new Lorentzians centered at zero, with opposite signs [Eq. (57)].

Back to point (c), now keeping the pump constant and increasing γ_a, we reach point (d). It is still in SC, although the cavity dissipation is very large (more than four times the coupling strength) for the small value of γ_b considered. Its spectrum of emission shows, however, a clear line splitting that is made neatly visible thanks to the cavity (residual) pumping P_a. Note that the actual separations of the two peaks are much larger than that of the dressed states. Increasing further the dissipation eventually brings the system into WC, but in region II where again due to $P_a \neq 0$, the spectrum remains a doublet. In Fig. 8(e), one can see, however, that there is no Rabi splitting and that the two peaks arise as a result of a subtraction of the two Lorentzians centered at $\omega_a=0$ [see the WC spectrum decomposition in Eqs. (50) and (57)]. Varying detuning for the system of point (e) even leads to an apparent anticrossing. Note that the transition from SC to WC is always smooth in the observed spectra, although it is an abrupt transition in terms of apparition or disappearance of dressed states (due to a change in sign in a radical in the underlying mathematical formalism).

If P_a is set to zero, i.e., in the case of a very clean sample with no spurious QDs other than the SC-coupled one, which experiences only an electronic pumping, region 3 of SC and II of WC disappear.[48] The former is indeed the result of the residual cavity photons helping SC. The "pathology" in WC of featuring two peaks at resonance also disappears, but most importantly, region 2 considerably increases inside the "triangle" of SC, meaning that the parameters required so that the line splitting can still be resolved in the luminescence spectrum now put much higher demands on the quality of the structure. This difficulty, especially in the region where $P_b \ll g$, follows from the "effective quantum state in the steady state" that we have already discussed. The presence of a cavity pumping, even if it is so small that no field-intensity effects are accounted for, can favor SC by making it visible, indeed by merely providing a photonlike character to the quantum state. This is the manifestation in a SS of the same

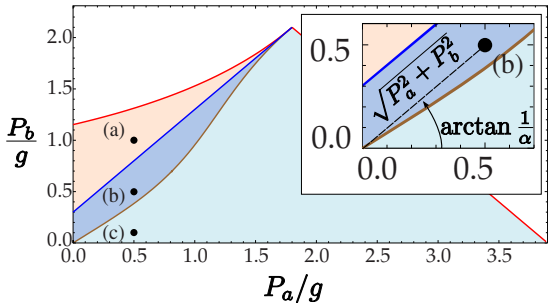

FIG. 10. (Color online) Phase space of SC/WC as a function of the pumps P_b/g and P_a/g for fixed decay parameters $\gamma_a=3.8g$ and $\gamma_b=0.1g$. As in Fig. 8, the red lines mark the physical regions and the blue one the SC (blue shades)/WC (red shades) transition, with the same regions 1 and 2 of SC and III of WC, also with the points (a)–(c), of Fig. 8. In the inset, zoom of the low-pump region, showing the importance of both the angle, $\arctan(1/\alpha)$, and the magnitude, $\sqrt{P_a^2+P_b^2}$, of a given point in the diagram.

influence that was observed in the SE; the luminescence spectrum of a photon as an initial state of the coupled system is more visible than that of an exciton, keeping all parameters otherwise the same (see Fig. 6).

A second useful picture to highlight this last point is that where the various regions are plotted in terms of the pumping rates, P_a and P_b (see Fig. 10, for lines (a)–(c) with $\gamma_a=3.8g$ in Fig. 8). The angle of a given point with the horizontal, linked to $\alpha^{-1}=P_b/P_a$, defines the excitonlike or photonlike character of the SS established in the system, and thus determines the visibility of the double-peak structure of SC. This is, at low pumpings, independent of the magnitude $\sqrt{P_a^2+P_b^2}$, as the brown line defined by Eq. (66) is approximately linear in this region. This shows the importance of a careful determination of the quantum state that is established in the SS by the interplay of the pumping and decay rates, through Eq. (12). The magnitude $\sqrt{P_a^2+P_b^2}$, on the other hand, affects the splitting $2R_0$, and the linewidth $2\Gamma_+$. In order to have a noticeable renormalization, the pumps must be comparable to the decays. On one hand, the Rabi frequency can be affected in different ways by the pumpings, depending on the parameters. If $\Gamma_a=\Gamma_b$, there is, in general, no effect of decoherence on the splitting of the dressed states, showing that in this case there is a perfect symmetric coupling of the modes into the new eigenstates (although the broadening can be large and spoil the resolution of the Rabi splitting anyway). If they are different, for example in the common situation that $\gamma_a-\gamma_b>P_a-P_b$, the Rabi increases with increasing P_a-P_b. On the other hand, the linewidth $2\Gamma_+=(\gamma_a+\gamma_b-P_a-P_b)/2$ presents clear bosonic characteristics; it increases with the decays but narrows with pumping.[31] The intensity of the pumps also affects the total intensity of the spectra, which is proportional to n_a^{SS} through γ_a and the integration time of the apparatus. Here, however, we have focused on the normalized spectra (i.e., the line shape).

VI. SUMMARY AND CONCLUSIONS

In conclusion, we have brought under a unified formalism the zero-dimensional light-matter interaction between bosons, both in the weak coupling (WC) and strong coupling (SC), for the two cases of spontaneous emission (SE) of an initial state and emission under a steady state (SS) maintained by an incoherent continuous pumping. While the SE case for some particular initial conditions (excited state of the atom) and configurations (resonance, direct emission) has been a pillar of SC in cavity quantum electrodynamics (cQED) of atoms in cavities, the extensions that we provided here to include a continuous and incoherent pumping are suitable to describe the recent field of cQED in semiconductor heterostructures. Together, they merge into an elegant and complementary theoretical edifice.

The main results of this paper are to be found in Eqs. (38)–(41) that provide the analytical expression for the cavity emission spectra of a system whose specificities—such as whether it corresponds to SE or the SS established by an incoherent continuous pumping—are provided by a parameter D, which, in the first (SE) case, is given by Eq. (42), and in the second (SS), by Eq. (45). These formulas, which allow for an arbitrary detuning between the bare modes, reduce to more self-contained expressions at resonance, namely, Eq. (52) for SE and Eq. (58) for SS. The resonance case allows an unambiguous definition of SC, depending on whether the complex Rabi frequency, Eq. (34), is pure imaginary (WC) or real (SC). This corresponds, in turn, to a damping or to sustained oscillations of the time autocorrelation of the fields. This is completely independent of the dynamics of the populations. SC is characterized by the emergence of new eigenstates, with different energies, whereas in WC, the energies remain degenerate. There is no, however, one-to-one mapping of this splitting of the energies with the lines observed in the luminescence spectrum. All cases can arise; one or two peaks can be observed at resonance both in WC and SC. In the SC case, one peak only is observed when the energy splitting is too small as compared to the broadening of the lines, whereas in the WC, two peaks are seen as a result of a resonance carving a hole in a single line, giving the illusion of a doublet (and indeed of an anticrossing when detuning is varied). For that reason, an understanding of the general picture is required to be able to position a particular experiment in the space of parameters, as was done in Figs. 8 and 10, rather than to rely on a qualitative effect of anticrossing at resonance. Figure 9 shows how loosely related are the observed line splitting in the luminescence spectrum (solid red) and the actual energy splitting of the polariton modes (dressed states, in dotted blue). The various situations that may arise are illustrated and discussed in Fig. 8. The respective effects of the angle and the distance to the origin in the P_a, P_b parameter space are shown in Fig. 10; the angle accounts for the effective quantum state that imparts on the visibility of the splitting in the spectrum, while the magnitude accounts for bosonic effects such as line narrowing and field-intensity renormalization of the Rabi splitting.

This work addresses the case of bosonic excitons with a linear model that also describes the so-called linear limit of vanishing excitation for a two-level exciton when it is far from saturation. As such, it also contains a lot of the physics of the ground state of quantum well excitons in planar cavities, although in this case, a direct polariton pumping must be taken into account, as particles are injected directly into

the ground state by scattering of other high-energy polaritons.[50] On the contrary, in our present scheme, the excitation is in terms of the bare modes, through phonon-assisted scattering of electron-hole pairs into the QD for the electronic pumping, P_b, or via Purcell emission of weakly coupled spectator dots into the cavity mode for the cavity pumping, P_a. A more natural extension of this work is to consider fermionic QDs that do not admit more than one exciton. In this case, the equations of motion for the correlators are not closed, and only semianalytical results are available. The structure of the spectra—that in the bosonic case decompose as a Lorentzian and a dispersive line for each peak—becomes that of an infinite series of lines, tightly grouped together, to give rise to multiplet structures in a wide variety of configurations. This fermionic case corresponds to mapping the Jaynes-Cummings ladder to an exact luminescence spectrum, in much the same way that we have been doing with the Rabi doublet in this text. This case, which is of crucial importance for the study of nonlinearity of genuine (two levels) QDs in semiconductor microcavities, is the subject of the second part of our work.[13]

ACKNOWLEDGMENTS

This work has been supported by the Spanish MEC under Contracts No. QOIT Consolider-CSD2006-0019, No. MAT2005-01388, and No. NAN2004-09109-C04-3 and by CAM under Contract No. S-0505/ESP-0200. E.d.V. acknowledges support of the FPU from the Spanish MEC.

*f.p.laussy@soton.ac.uk

[1] E. M. Purcell, Phys. Rev. **69**, 681 (1946).
[2] D. Kleppner, Phys. Rev. Lett. **47**, 233 (1981).
[3] P. Goy, J. M. Raimond, M. Gross, and S. Haroche, Phys. Rev. Lett. **50**, 1903 (1983).
[4] J.-M. Gérard, B. Sermage, B. Gayral, B. Legrand, E. Costard, and V. Thierry-Mieg, Phys. Rev. Lett. **81**, 1110 (1998).
[5] A. Kiraz, P. Michler, C. Becher, B. Gayral, A. Imamoglu, L. Zhang, and E. Hu, Appl. Phys. Lett. **78**, 3932 (2001).
[6] G. Khitrova, H. M. Gibbs, M. Kira, S. W. Koch, and A. Scherer, Nat. Phys. **2**, 81 (2006).
[7] J. P. Reithmaier, Semicond. Sci. Technol. **23**, 123001 (2008).
[8] J. J. Hopfield, Phys. Rev. **112**, 1555 (1958).
[9] E. Jaynes and F. Cummings, Proc. IEEE **51**, 89 (1963).
[10] S. Rudin and T. L. Reinecke, Phys. Rev. B **59**, 10227 (1999).
[11] R. H. Dicke, Phys. Rev. **93**, 99 (1954).
[12] M. Bienert, W. Merkel, and G. Morigi, Phys. Rev. A **69**, 013405 (2004).
[13] E. del Valle, F. P. Laussy, and C. Tejedor, following paper, Phys. Rev. B **79**, 235326 (2009).
[14] E. del Valle, F. P. Laussy, F. M. Souza, and I. A. Shelykh, Phys. Rev. B **78**, 085304 (2008).
[15] H. J. Carmichael, *Statistical Methods in Quantum Optics 1*, 2nd ed. (Springer, New York, 2002).
[16] H. J. Carmichael, R. J. Brecha, M. G. Raizen, H. J. Kimble, and P. R. Rice, Phys. Rev. A **40**, 5516 (1989).
[17] C. Weisbuch, M. Nishioka, A. Ishikawa, and Y. Arakawa, Phys. Rev. Lett. **69**, 3314 (1992).
[18] S. Pau, G. Björk, J. Jacobson, H. Cao, and Y. Yamamoto, Phys. Rev. B **51**, 14437 (1995).
[19] V. Savona, L. C. Andreani, P. Schwendimann, and A. Quattropani, Solid State Commun. **93**, 733 (1995).
[20] G. S. Agarwal and R. R. Puri, Phys. Rev. A **33**, 1757 (1986).
[21] L. C. Andreani, G. Panzarini, and J.-M. Gérard, Phys. Rev. B **60**, 13276 (1999).
[22] G. Cui and M. G. Raymer, Phys. Rev. A **73**, 053807 (2006).
[23] A. Naesby, T. Suhr, P. T. Kristensen, and J. Mork, Phys. Rev. A **78**, 045802 (2008).
[24] M. Yamaguchi, T. Asano, and S. Noda, Opt. Express **16**, 18067 (2008).
[25] S. Hughes and P. Yao, Opt. Express **17**, 3322 (2009).
[26] A. Auffèves, B. Besga, J.-M. Gérard, and J.-P. Poizat, Phys. Rev. A **77**, 063833 (2008).
[27] J. I. Inoue, T. Ochiai, and K. Sakoda, Phys. Rev. A **77**, 015806 (2008).
[28] L. V. Keldysh, V. D. Kulakovskii, S. Reitzenstein, M. N. Makhonin, and A. Forchel, Pis'ma Zh. Eksp. Teor. Fiz. **84**, 584 (2006).
[29] G. W. Gardiner, *Quantum Noise* (Springer-Verlag, Berlin, 1991).
[30] N. Averkiev, M. Glazov, and A. Poddubny, JETP **135**, 959 (2009).
[31] M. O. Scully and M. S. Zubairy, *Quantum Optics* (Cambridge University Press, Cambridge, England, 2002).
[32] E. del Valle, Ph.D. thesis, Universidad Autónoma de Madrid, 2009, http://delvalle.laussy.org/elena/thesis
[33] R. Alicki, Phys. Rev. A **40**, 4077 (1989).
[34] L. Mandel and E. Wolf, *Optical Coherence and Quantum Optics* (Cambridge University Press, Cambridge, England, 1995).
[35] J. Eberly and K. Wódkiewicz, J. Opt. Soc. Am. **67**, 1252 (1977).
[36] E. del Valle, F. P. Laussy, F. Troiani, and C. Tejedor, Phys. Rev. B **76**, 235317 (2007).
[37] J. P. Reithmaier, G. Sek, A. Löffler, C. Hofmann, S. Kuhn, S. Reitzenstein, L. V. Keldysh, V. D. Kulakovskii, T. L. Reinecker, and A. Forchel, Nature (London) **432**, 197 (2004).
[38] T. Yoshie, A. Scherer, J. Heindrickson, G. Khitrova, H. M. Gibbs, G. Rupper, C. Ell, O. B. Shchekin, and D. G. Deppe, Nature (London) **432**, 200 (2004).
[39] E. Peter, P. Senellart, D. Martrou, A. Lemaître, J. Hours, J. M. Gérard, and J. Bloch, Phys. Rev. Lett. **95**, 067401 (2005).
[40] K. Hennessy, A. Badolato, M. Winger, D. Gerace, M. Atature, S. Gulde, S. Fält, E. L. Hu, and A. Imamoglu, Nature (London) **445**, 896 (2007).
[41] D. Press, S. Götzinger, S. Reitzenstein, C. Hofmann, A. Löffler, M. Kamp, A. Forchel, and Y. Yamamoto, Phys. Rev. Lett. **98**, 117402 (2007).
[42] S. Reitzenstein, C. Hofmann, A. Gorbunov, M. Strauß, S. H. Kwon, C. Schneider, A. Löffler, S. Höfling, M. Kamp, and A. Forchel, Appl. Phys. Lett. **90**, 251109 (2007).
[43] A. Faraon, I. Fushman, D. Englund, N. Stoltz, P. Petroff, and J. Vuckovic, Nat. Phys. **4**, 859 (2008).
[44] M. Nomura, Y. Ota, N. Kumagai, S. Iwamoto, and Y. Arakawa,

Appl. Phys. Express **1**, 072102 (2008).
[45] A. Laucht, F. Hofbauer, N. Hauke, J. Angele, S. Stobbe, M. Kaniber, G. Böhm, P. Lodahl, M.-C. Amann, and J. J. Finley, New J. Phys. **11**, 023034 (2009).
[46] A. Dousse, J. Suffczyński, R. Braive, A. Miard, A. Lemaître, I. Sagnes, L. Lanco, J. Bloch, P. Voisin, and P. Senellart, Appl. Phys. Lett. **94**, 121102 (2009).
[47] S. M. Thon, M. T. Rakher, H. Kim, J. Gudat, W. T. M. Irvine, P. M. Petroff, and D. Bouwmeester, Appl. Phys. Lett. **94**, 111115 (2009).
[48] F. P. Laussy, E. del Valle, and C. Tejedor, Phys. Rev. Lett. **101**, 083601 (2008).
[49] F. P. Laussy, E. del Valle, and C. Tejedor, arXiv:0808.3215, to be published in AIP Conference Proceedings ICPS28.
[50] F. P. Laussy, G. Malpuech, A. Kavokin, and P. Bigenwald, Phys. Rev. Lett. **93**, 016402 (2004).